Biosensors and Bioelectronics 26 (2011) 2473–2477

Contents lists available at ScienceDirect

Biosensors and Bioelectronics

journal homepage: www.elsevier.com/locate/bios

Au-NPs enhanced SPR biosensor based on hairpin DNA without the effect of nonspecific adsorption

Qingfen Luan[a], Kebin Zhou[a], Haina Tan[a], Dan Yang[a], Xin Yao[a,b,*]

[a] College of Chemistry and Chemical Engineering, Graduate University of Chinese Academy of Sciences, Beijing 100049, PR China
[b] State Key Laboratory of Natural and Biomimetic Drugs, Peking University, Beijing 100191, PR China

ARTICLE INFO

Article history:
Received 21 June 2010
Received in revised form 22 October 2010
Accepted 22 October 2010
Available online 30 October 2010

Keywords:
Gold nanoparticles
Hairpin DNA
Surface plasmon resonance
*Rsa*I endonuclease
Nonspecific adsorption

ABSTRACT

Gold nanoparticles (Au-NPs) are usually used to amplify surface plasmon resonance (SPR) signals, however, the serious nonspecific adsorption has largely limited their practical applications. Here, we developed a novel Au-NPs enhanced biosensor without the effect of nonspecific adsorption: cutting Au-NPs off from the biosensor surface by *Rsa*I endonuclease. In order to further improve the sensitivity, the probe DNA was designed specially. After the cleavage reaction, the residual probe DNA formed hairpin structure, which also resulted in a great change in SPR dip shift. Then, with the coaction of Au-NPs and conformation change of probe DNA, the SPR signal was amplified greatly. Using this method, we monitored the process of DNA cleavage in real-time and achieved a detection level of 5×10^{-8} M. Moreover, the result of X-ray photoelectron spectroscopy (XPS) experiment further confirmed that large nonspecific adsorption existed. However, because SPR recorded a process in which the Au-NPs were cut off, the serious nonspecific adsorption did not affect the experimental result.

1. Introduction

Recently, surface plasmon resonance (SPR) as a viable analytical method for the rapid, sensitive and label-free bioanalysis has received extensive attentions (Baird et al., 2002; Kindermann et al., 2003; Shumaker-Parry et al., 2004; Su et al., 2008; Vutukuru et al., 2006; Wink et al., 1998). For all that, most of the conventional SPR instruments are not able to measure extremely small changes in refractive index which hinders their practical applications in ultrasensitive detection (He et al., 2000). To overcome this disadvantage, various amplification strategies such as polymerase chain reaction (PCR)-amplified, enzymatically amplified and gold nanoparticles (Au-NPs) enhanced methods have been utilized in conjunction with SPR (Carrascosa et al., 2009; Goodrich et al., 2004; Wang et al., 2009; Yao et al., 2006). Among them, Au-NPs as popular and useful labels for amplifying weak signals have been widely adopted (Matsui et al., 2005; Riskin et al., 2009; Wang et al., 2009; Yao et al., 2006). For instance, Lyon et al. (1998) have developed a type of Au-amplified SPR sandwich immunoassay achieving a picomolar detection of human immunoglobulin G, and they also conducted systematic studies of the effect of gold particle size and surface coverage on SPR response (Lyon et al., 1999a,b). He et al. (2000) further extended the scope of Au-amplified SPR to the analysis of DNA hybridization, however, according to the reference, there was about 40% of the nonspecific adsorption without blocker, and the SPR signal enhancement was largely limited by nonspecific adsorption of Au-NPs onto the sensor surfaces (He et al., 2000). To circumvent this problem, He et al. (2000) further used polyethylene glycol (PEG) to reduce the nonspecific adsorption of Au-NPs while there was still approximately 10% of the unwanted interference. Wang and coworkers used SiO_2 layer and layer-by-layer (LBL) assembly films of (PAH/PSS) as the shield to prevent the metal deposition in the process of catalytic growth of Au-NPs successively. Nevertheless, nanometer thickness of SiO_2 layer was easy to crack, and the preparations of SiO_2 layer or LBL-coated Au film were time-consuming, high-cost and could not decrease nonspecific adsorption effectively (Wang et al., 2007; Yang et al., 2007). In our previous study, carboxylated dextran had been attempted to decrease nonspecific adsorption, in which though the nonspecific adsorption has been effectively avoided, the experimental process was complicated and the reproducibility was not very good (Yao et al., 2006). Therefore, developing methods which cannot only make the best of Au-NPs to amplify the SPR signal but also avoid the effect of nonspecific adsorption is necessary.

In this paper, we developed a novel type of Au-NPs enhanced SPR biosensor without the effect of nonspecific adsorption by cutting Au-NPs off from the biosensor surface. In order to further improve the sensitivity, a hairpin DNA was also introduced into the

* Corresponding author at: College of Chemistry and Chemical Engineering, Graduate University of Chinese Academy of Sciences, Beijing 100049, PR China.
Tel.: +86 10 88256414; fax: +86 10 88256092.
E-mail address: yaox@gucas.ac.cn (X. Yao).

0956-5663/$ – see front matter © 2010 Elsevier B.V. All rights reserved.
doi:10.1016/j.bios.2010.10.035

system. Hairpin DNAs are single-stranded DNAs with a stem–loop structure, and have been found to exhibit good stability, high sensitivity and excellent specificity. Due to these advantages, hairpin DNAs have been used for many applications including DNA/DNA, DNA/RNA studies and DNA–protein interaction assays (Fan et al., 2003; Li et al., 2008b; Liu et al., 2008; Tan et al., 2004). The traditional methods for studying hairpin DNAs are based on fluorescent and electrochemical measurements. In these studies, it was found that there is a conformation change of hairpin DNA during the detection process (Benson et al., 2004; Chen et al., 2002; Liu et al., 2005; Vacek et al., 2008; Zauner et al., 2005). By taking advantage of this conformation change, we firstly realized the hairpin DNAs study using SPR and found that the conformation change of hairpin DNAs can result in a large change in SPR dip shift (Luan et al., 2010a,b). Here, we further extended this strategy for real-time monitoring of double-stranded DNA cleavage by using *Rsa*I endonuclease, a restriction endonuclease, which recognizes the GTAC sequence as a model target. Restriction endonucleases are one of the most important enzymes in molecular biology. They are essential in recombinant technology, genotyping, mapping, and sequencing of large strands of DNA (Bhagwat, 1992; Pingoud, 2001). Because of the biological importance of restriction endonucleases and their wide use, restriction endonuclease activity assays are essential. *Rsa*I endonuclease as an important restriction endonuclease has caught more and more attentions recently (Ma et al., 2007, 2008). The experimental results demonstrated that the SPR signal was amplified greatly with the coaction of Au-NPs and the conformation of hairpin DNAs. Using this method, the process of DNA cleavage in real-time was monitored and a very low detection level of 5×10^{-8} M was obtained. Additionally, though the result of X-ray photoelectron spectroscopy (XPS) experiment further confirmed that large nonspecific adsorption existed, such nonspecific adsorption did not affect the experimental result because SPR recorded a process in which the Au-NPs were cut off.

2. Experimental

2.1. Materials and reagents

*Rsa*I endonuclease and *Eco*RI endonuclease were purchased from New England Biolabs, Inc. (NEB). The DNA sequences for probes and target were: Probe DNA1 (5′-SH-$(CH_2)_6$-TTTTTT-*ACCGTG*-TTTT-*CACGGT*-ACGGATACTA-3′), Probe DNA2 (5′-SH-$(CH_2)_6$-TTTTTT-CTGAGC-TTTT-CACGGT-ACGGATACTA-3′); complementary target DNA (cDNA) (5′-SH-$(CH_2)_6$-TAGTATCCGTAC-3′). The sequences in italics in probe DNA1 represented the stem of hairpin DNA; cDNA was complementary with 12 bases from 3′ end of probe DNAs. All of the sequences were purchased from Shanghai Shenggong Biotechnology Co. (Shanghai, China), and used without further purification. *Rsa*I endonuclease and *Eco*RI endonuclease stock solutions were prepared with 50 mM Tris–HCl buffer solution containing 5 mM $MgCl_2$ (pH 8.0); the probe DNAs and cDNA stock solutions were prepared with 10 mM phosphate buffer solution (PBS, pH 7.0) containing 0.3 M NaCl. 6-mercapto-1-hexanol (MCH) was acquired from Sigma (USA), $AuCl_3 \cdot HCl \cdot 4H_2O$ was purchased from Sinopharm Chemical Reagent Co., Ltd. (Shanghai, China). Trisodium citrate and other reagents used were all obtained from Beijing Chemical Reagents Co. (Beijing, China). Millipore Milli Q (18 MΩ cm) water was used in all experiments.

2.2. Preparation of SPR sensor surface

Au-NPs (13-nm diameter) were synthesized and modified according to the procedures described by Storhoff et al. (1998). The fabrication and modification of SPR sensor were carried out as follows. The BK7 glass slides (Fisher) were heated in a piranha solution (30% H_2O_2 and 70% concentrated H_2SO_4) at 80 °C for 30 min (Caution: piranha solution is strongly oxidizing and should be handed carefully!). Upon cooling to room temperature, the glass slides were rinsed thoroughly with deionized water. Before the preparation of gold substrate, the slides were dried by N_2 steam. The gold substrate was obtained by evaporating 50-nm thick gold on glass slides which had been previously coated with a 2 nm Cr layer by a sputtering coater (Model 108, Kert J. Lester Inc., Clairton, PA).

For each concentration experiment of endonuclease, 20 μl of 1 μM probe DNA solution was dropped onto the pretreated film and incubated overnight at 4 °C. After rinsed with PBS and dried with N_2, the modified film was blocked by 1.45×10^{-5} M MCH for 3 min. Then 20 μl of 200 nM Au-NPs labeled cDNA solution was dropped onto the modified film and allowed to react for 3 h. Finally, the modified films were rinsed with water thoroughly, dried with N_2 and prepared for the SPR measurement.

2.3. Apparatus and measurements

The home-built FI-SPR instrument, equipped with a bi-cell detector for high-resolution measurements, has been described elsewhere (Luan et al., 2010a,b; Song et al., 2002; Yao et al., 2006, 2004, 2007). Briefly, the SPR instrument recorded reflected light falling onto the two cells at two (A and B) of photodetectors, then both the differential (A − B) and the sum (A + B) signals were recorded by a PCI-1731 interface card (Advantech, Taiwan) controlled by a Labview program. The ratio of the differential to sum signals, which is linearly proportional to the SPR angular shift, was obtained numerically by dividing (A − B) with (A + B) (Song et al., 2002; Yao et al., 2004, 2007). To convert the ratio of (A − B)/(A + B) to the SPR dip shift, an instrumental calibration experiment was carried out using a method similar to that reported by Kolomenskii et al. (1997). The incorporation of a bi-cell photodiode detector to measure the differential signal resulted in a much-improved angular resolution (10^{-4} to 10^{-5} degrees) (Song et al., 2002; Tao et al., 1999). All of the endonuclease solutions were introduced into the Tris–HCl carrier solution by a 50-μl sample loop on a six-port valve and subsequently were delivered to the flow cell at a constant speed of 1.0 mL/h by a syringe pump (KDS100, KD Scientific Inc., Holliston, MA, USA). After the cleavage reaction, the SPR sensor surface was washed by Tris–HCl carrier solution and the SPR spectra was recorded during the whole process.

High-resolution transmission electron microscope (HRTEM) JEM-2010 was used to reveal the size and monodispersity of Au-NPs.

X-ray photoelectron spectroscopy (XPS) data were obtained with an ESCALab220i-XL electron spectrometer (VG Scientific) using 300 W Al Kα radiation. The base pressure was about 3×10^{-9} mbar. The binding energies were referenced to the C 1s line at 284.8 eV from adventitious carbon.

3. Results and discussion

3.1. The experimental principle

Fig. 1 illustrates the principle of the present method. After being immobilized on Au film, probe DNA1 was hybridized with 13 nm Au-NPs labeled cDNA. When encountered with *Rsa*I endonuclease, the hybridized double-strand DNAs were cleaved, Au-NPs were cut off and the residual probe formed hairpin structure. As a result, the coaction of Au-NPs and conformation change of hairpin DNA

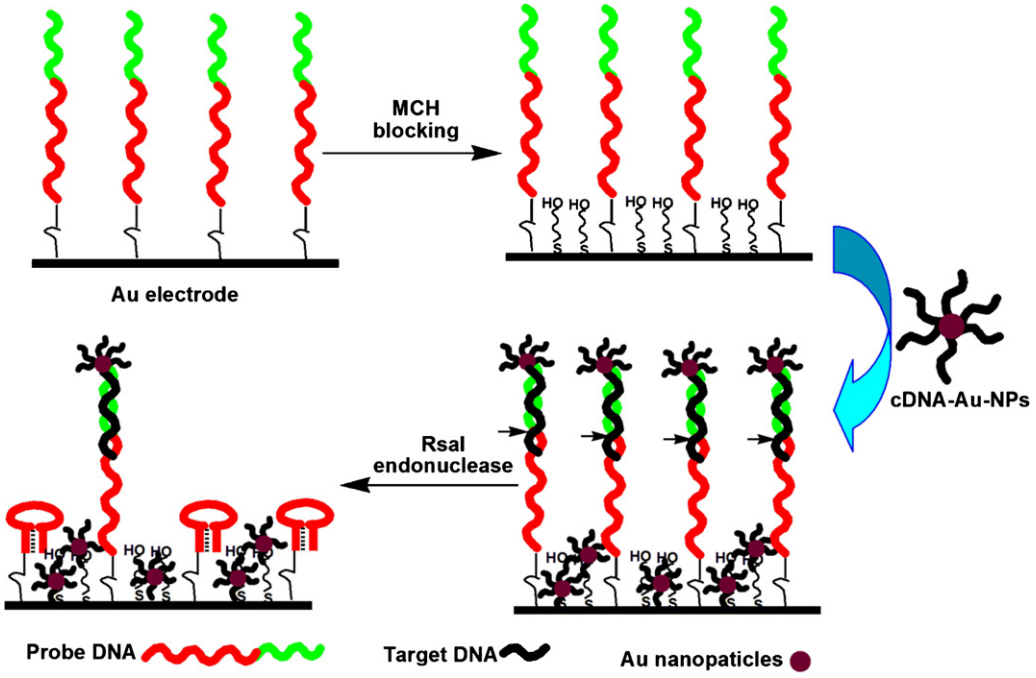

Fig. 1. Principle scheme of monitoring activity of *Rsa*I endonuclease with the coaction of Au-NPs and hairpin DNA. For clarity, all of the molecules were not drawn to scale.

resulted in a great change in SPR dip shift that could be recorded in situ.

Fig. 2 shows the SPR response on injection of 200 nM Au-NPs labeled cDNA onto the Au film which has been modified by 1.45×10^{-5} M MCH for 12 h previously. As soon as the Au-NPs were in contact with the modified film (~150 s), an increase of the SPR signal can be observed, which can be attributed to the Au-NPs labeled cDNA adsorbed onto the Au film. Moreover, when Au-NPs achieved the surface of the Au film, some of them were unstable and can be eluted by the buffer. This repeated elution and adsorption process resulted in the bumps in the signal curve. Once the injected Au-NPs completely eluted out of the cell (~330 s), the signal decreases, which may result from the desorption of some unstable nonspecific Au-NPs from Au film (Carrascosa et al., 2009; Song et al., 2002). The net SPR signal changes greatly (0.0096°) indicating that the nonspecific adsorption is very serious with the use of MCH as a blocker.

The large nonspecific adsorption also can be found from the XPS data (Fig. 3). Considering that characterizing Au-NPs on Au film is difficult, Ag film was used as the substrate in the experiment. From curve a, it can be seen that there is no Au-NPs on bare Ag film. After the Au-NPs labeled cDNA was dropped onto the MCH modified (12 h) Ag film and kept still for 3 h, there is a serious nonspecific adsorption (curve b) and the relative atomic percentage (At) of Au-NPs is about 0.11%. At can be obtained from the following formula:

$$\mathrm{At} = \frac{I_i/S_i}{\sum I_i/S_i} \times 100\%$$

where I_i is the peak intensity of i element; S_i is the relative element sensitivity factor of i element. After hybridized with the labeled cDNA, about 0.16% Au-NPs are immobilized onto the film (curve c). Some of the whole immobilized Au-NPs are confined

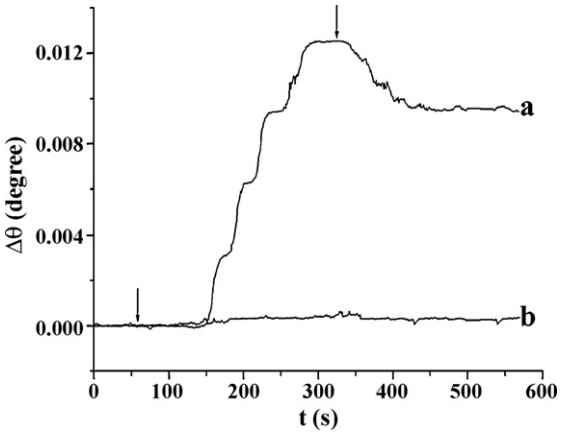

Fig. 2. SPR response on injecting 200 nM Au-NPs labeled cDNA to the Au film modified by 1.45×10^{-5} M MCH for 12 h previously. PBS was used as the carrier solution. The arrow indicated the time when the samples were injected to the flow cell and the time when washing was done.

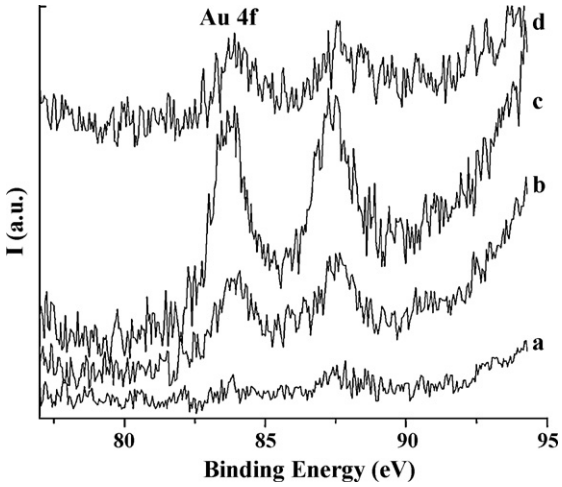

Fig. 3. Au 4f XPS spectra for (a) bare Ag film, (b) MCH and Au-NPs labeled cDNA modified Ag film, (c) probe DNA1, MCH and Au-NPs labeled cDNA modified Ag film, (d) after c film exposure to the *Rsa*I endonuclease.

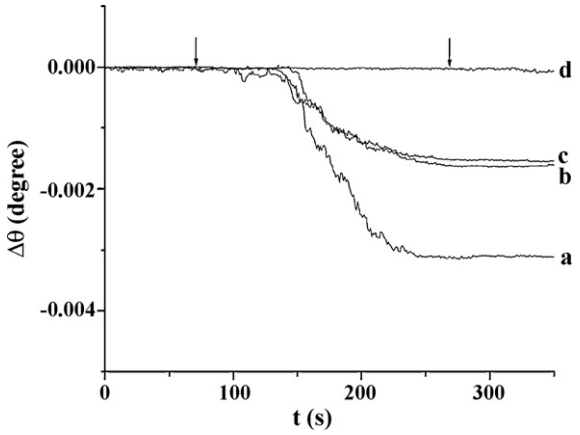

Fig. 4. SPR responses on injecting 1 μM *Rsa*I endonuclease for: probe DNA1 modified Au surface hybridized to with (a) or without (c) Au-NPs labeled cDNA, probe DNA2 modified Au surface hybridized to Au-NPs labeled cDNA (b); Curve d was SPR responses on injecting 1 μM *Eco*RI endonuclease for probe DNA1 modified Au surface hybridized to Au-NPs labeled cDNA. Tris–HCl was used as the carrier solution. The arrow indicated the time when the samples were injected to the flow cell and the time when washing was done.

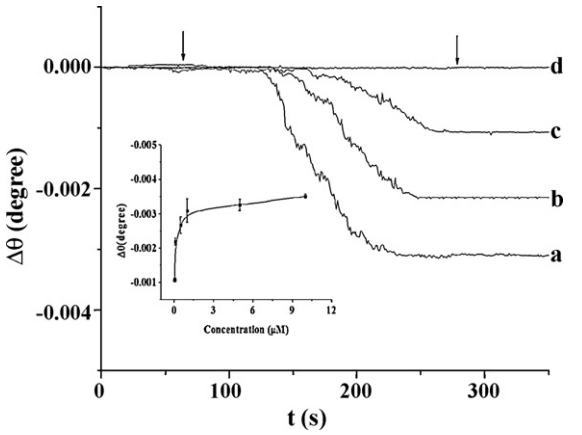

Fig. 5. SPR responses of the probe DNA1 Au surface after hybridized to Au-NPs labeled cDNA on injecting different *Rsa*I endonuclease concentration: (a) 1 μM, (b) 0.1 μM, (c) 0.05 μM and (d) 0 μM. The inset showed SPR responses plotted as a function of *Rsa*I endonuclease concentration from 0.05 to 10 μM. The standard deviations were computed from at least three replicate measurements and shown as the error bars. The arrow indicated the time when the samples were injected to the flow cell and the time when washing was done.

by hybridization, while the others are introduced by nonspecific adsorption. After the cleavage reaction, because the concentration of *Rsa*I endonuclease is quite high (1.0×10^{-5} M) and the action time is long (0.5 h), Au-NPs immobilized by hybridization have been almost cut off (from curve c to curve d). In addition, from curve d it also can be seen that about 0.11% Au-NPs are still on the film, which is consistent with the quantity of the Au-NPs introduced by nonspecific adsorption (curve b). This result further confirms that there is a serious nonspecific adsorption in the experimental process (~68%). However, SPR recorded the process in which the Au-NPs were cut off (from curve c to curve d). Therefore, the effect of nonspecific adsorption was avoided efficiently and a novel enhanced SPR biosensor was developed.

3.2. SPR signal amplification

In order to further clarify the advantages of Au-NPs amplification on *Rsa*I endonuclease assay, a comparing experiment was carried out and the result is shown in Fig. 4. It can be seen that the SPR signal change with Au-NPs amplification (curve a) is approximately twice as much as that without Au-NPs enhancement (curve c), demonstrating that Au-NPs greatly amplified SPR signal. This result can be attributed to the combined effect of great decreases of the surface mass, refractive index and electromagnetic coupling between Au-NPs and Au film (He et al., 2000) when Au-NPs are cut off by *Rsa*I endonuclease. Specifically, due to the higher mass and larger dielectric constant than that of the biomolecules, Au-NPs can result in a higher index change and then caused a larger SPR signal change. Moreover, binding of Au-NPs to Au film can lead to large changes in SPR reflectivity through strong electromagnetic coupling between Au film and Au-NPs due to the interactions between the surface plasmons of the Au film and the localized surface plasmons (LSP) of Au-NPs (He et al., 2000; Lyon et al., 1999a,b; Manera et al., 2010).

According to our previous study, the conformation change of hairpin DNA can also result in a large SPR signal change (Luan et al., 2010a,b). To confirm the advantage of hairpin DNA in the present system, another experiment was conducted. Au-NPs labeled cDNA was used as the target DNA, and the probe DNAs were different: after reacted with *Rsa*I endonuclease, probe DNA1 could be converted to hairpin structure, but probe DNA2 would be still linear structure because its base sequence of 5′ was adjusted to avoid forming hairpin DNA. From Fig. 4, it can be seen that the sensitivity of probe DNA1 (curve a) is greater than that of probe DNA2 (curve b). This result can be explained that after reacted with *Rsa*I endonuclease, the rest part of probe DNA1 can change from linear helix to loop–stem structure, which induces a larger conformation change and results in a larger SPR dip shift change than that caused by probe DNA2. The result is also consistent with our previous study which has found that because of the larger conformation change, hairpin DNA resulted in a greater SPR signal change than linear DNA (Luan et al., 2010b).

To further demonstrate that SPR signal change was caused by the specific cleavage reaction, another control experiment has also been carried out. *Eco*RI endonuclease which recognizes the GAATTC sequence was chosen as the negative restriction endonuclease. Because there is no sequence recognized by *Eco*RI endonuclease in the present system, no SPR signal change occurs during the injection of *Eco*RI endonuclease to the probe DNA1 modified Au surface after probe DNA1 hybridizing to the AuNPs labeled cDNA (curve d, in Fig. 4).

Then, combining Au-NPs with hairpin DNA, the SPR signal was greatly improved. So we used this signal amplified system to complete the *Rsa*I endonuclease assay.

3.3. The assay of RsaI endonuclease

Fig. 5 depicts time-resolved SPR dip shift curves acquired by injecting *Rsa*I endonuclease at 0 M (curve d), 5×10^{-8} M (curve c), 1×10^{-7} M (curve b) and 1×10^{-6} M (curve a) to the modified films. The net dip shift in curve c is approximately 0.001° greater than that shown in curve d which indicates that 5×10^{-8} M *Rsa*I endonuclease could be measured by our high-resolution SPR instrument. SPR signals increase with the increasing concentrations of *Rsa*I endonuclease, which suggests that the method could be used for quantitative measurements of *Rsa*I endonuclease. To display this trend more clearly, the dose-dependent curve plotted from 5×10^{-8} M to 1×10^{-5} M is also given (inset in Fig. 5). The relative standard deviations (RSD), shown as the error bars in the figure, are all <10% which could be acceptable among the typical analytical techniques (Skong et al., 1998). Notice, the slope of the inset in Fig. 5 is steeper between 5×10^{-8} and 1×10^{-6} M, however, around 1×10^{-6} M the curve begins to level off which probably

aroused from the fact that most of the double-strand DNAs have been reacted with *Rsa*I endonuclease. Even if the *Rsa*I endonuclease concentration continues to increase, the change of SPR signal becomes very small. Moreover, because more double strand DNA were immobilized on the Au film and the sensitivity of this method is very high, the *Rsa*I endonuclease concentration which can be detected is very low. The maximum concentration in Fig. 5 is still not enough to react with all double strand DNAs, so the curve does not lead to a constant plateau.

In addition, the high sensitivity is one of the advantages of our method, as mentioned above. From Fig. 5, we found the detection level for *Rsa*I endonuclease was quite low (5×10^{-8} M). The amount of sample needed per analysis was only 50 μl. The *Rsa*I endonuclease in such a small sample volume corresponds to 2.5×10^{-12} mol. Moreover, the limit of detection (LOD) was 5×10^{-10} M, which was the concentration when the SPR signal was $3 \times$ SNR (signal to noise ratio). Such a detection value is far lower than those of measurements based on electrochemistry and fluorescence (Jin, 2009; Li et al., 2008a; Ma et al., 2007, 2008; Huang and Quiñones, 2008). Such a decrease is attributable to the signal amplified effect caused by the coaction of Au-NPs and conformation change of hairpin DNA. To be specific, during the double-strand DNA cleavage process, Au-NPs are cut off and probe DNA1 converts from a linear helix to a loop–stem structure, both of which can also lead to a greater change in SPR dip shift. Besides that, such a low detection level may be partly due to the high sensitivity of our home-built SPR instrument which takes a bi-cell photodiode detector to measure the differential signal and owns a much-improved angular resolution.

4. Conclusion

In summary, combining Au-NPs with hairpin DNA, a sensitive and simple method for the activity assay of *Rsa*I endonuclease was developed. In the present system, the SPR signals can be amplified by both Au-NPs and the conformation change of hairpin DNA. Using this method, the process of DNA cleavage in real-time was monitored and a detection level of 5×10^{-8} M was obtained, which was far lower than those obtained by electrochemical and fluorescent measurements. Moreover, though the result of XPS experiment demonstrated that large nonspecific adsorption existed, the serious nonspecific adsorption did not affect the experimental result, because SPR recorded a process in which the Au-NPs were cut off.

Acknowledgements

This work was supported by grants from National Natural Science Foundation of China (20703065 and 20877097), the Ministry of Science and Technology of China (2008AA06Z324), the Ministry of Science and Technology of China (973 program 2010CB833101).

References

Baird, C.L., Courtenay, E.S., Myszka, D.G., 2002. Anal. Biochem. 310, 93–99.
Benson, E.L., Tomich, P.K., Wolfe, M.L., Choi, G.H., Hagadorn, J.C., Mutchler, V.T., Garlick, R.L., 2004. Anal. Biochem. 324, 298–300.
Bhagwat, A.S., 1992. Methods Enzymol. 216, 199–224.
Carrascosa, L.G., Calle, A., Lechuga, L.M., 2009. Anal. Bioanal. Chem. 393, 1173–1182.
Chen, X.C., Hentz, N.G., Hubbard, F., Meier, T.I., Sittampalam, S., Zhao, G., 2002. Anal. Biochem. 309, 232–240.
Fan, C.H., Plaxco, K.W., Heeger, A.J., 2003. Proc. Natl. Acad. Sci. U.S.A. 100, 9134–9137.
Goodrich, T.T., Lee, H.J., Corn, R.M., 2004. J. Am. Chem. Soc. 126, 4086–4087.
He, L., Musick, M.D., Nicewarner, S.R., Salinas, F.G., Benkovic, S.J., Natan, M.J., Keating, C.D., 2000. J. Am. Chem. Soc. 122, 9071–9077.
Huang, Q., Quiñones, E., 2008. Anal. Biochem., doi:10.1016/j.ab.2008.1004.1038.
Jin, Y., 2009. Anal. Chim. Acta 634, 44–48.
Kindermann, M., George, N., Johnsson, N., Johnsson, K., 2003. J. Am. Chem. Soc. 125, 7810–7811.
Kolomenskii, A.A., Gershon, P.D., Schuessler, H.A., 1997. Appl. Opt. 36, 6539–6547.
Li, X.M., Song, C., Zhao, M.P., Li, Y.Z., 2008a. Anal. Biochem. 381, 1–7.
Li, Y.S., Zhou, X.Y., Ye, D.Y., 2008b. Biochem. Biophys. Res. Commun. 373, 457–461.
Liu, G., Wan, Y., Gau, V., Zhang, J., Wang, L.H., Song, S.P., Fan, C.H., 2008. J. Am. Chem. Soc. 130, 6820–6825.
Liu, L.F., Tang, Z.W., Wang, K.M., Tan, W.H., Li, J., Guo, Q.P., Meng, X.X., Ma, C.B., 2005. Analyst 130, 350–357.
Luan, Q.F., Xue, Y., Yao, X., 2010a. Analyst 135, 414–418.
Luan, Q.F., Xue, Y., Yao, X., 2010b. Sens. Actuators B Chem. 147, 561–565.
Lyon, L.A., Musick, M.D., Natan, M.J., 1998. Anal. Chem. 70, 5177–5183.
Lyon, L.A., Musick, M.D., Smith, P.C., Reiss, B.D., Pena, D.J., Natan, M.J., 1999a. Sens. Actuators B Chem. 54, 118–124.
Lyon, L.A., Pena, D.J., Natan, M.J., 1999b. J. Phys. Chem. B 103, 5826–5831.
Ma, C.B., Tang, Z.W., Huo, X.Q., Yang, X.H., Li, W., Tan, W.H., 2008. Talanta 76, 458–461.
Ma, C.B., Tang, Z.W., Wang, K.M., Tan, W.H., Yang, X.H., Li, W., Li, Z.H., Lv, X.Y., 2007. Anal. Biochem. 363, 294–296.
Manera, M.G., Spadavecchia, J., Taurino, A., Rella, R., 2010. J. Opt. 12, 035003.
Matsui, J., Akamatsu, K., Hara, N., Miyoshi, D., Nawafune, H., Tamaki, K., Sugimoto, N., 2005. Anal. Chem. 77, 4282–4285.
Pingoud, A., 2001. Nucleic Acids Res. 29, 3705–3727.
Riskin, M., Tel-Vered, R., Lioubashevski, O., Willner, I., 2009. J. Am. Chem. Soc. 131, 7368–7378.
Shumaker-Parry, J.S., Aebersold, R., Campbell, C.T., 2004. Anal. Chem. 76, 2071–2082.
Skong, D.A., Holler, F.J., Nieman, T.A., 1998. Principles of Instrumental Analysis. Harcourt Brace, Philadelphia.
Song, F.Y., Zhou, F.M., Wang, J., Tao, N.J., Lin, J.Q., Vellanoweth, R.L., Morquecho, Y., Wheeler-Laidman, J., 2002. Nucleic Acids Res. 30, e72.
Storhoff, J.J., Elghanian, R., Mucic, R.C., Mirkin, C.A., Letsinger, R.L., 1998. J. Am. Chem. Soc. 120, 1959–1964.
Su, X.D., Neo, S.J., Peh, W.Y.X., Thomsen, J.S., 2008. Anal. Biochem. 376, 137–143.
Tan, W.H., Wang, K.M., Drake, T.J., 2004. Curr. Opin. Chem. Biol. 8, 547–553.
Tao, N.J., Boussaad, S., Huang, W.L., Arechabaleta, R.A., D'Agnese, J., 1999. Rev. Sci. Instrum. 70, 4656–4660.
Vacek, J., Cahova, K., Palecek, E., Bullard, D.R., Lavesa-Curto, M., Bowater, R.P., Fojta, M., 2008. Anal. Chem. 80, 7609–7613.
Vutukuru, S., Bethi, S.R., Kane, R.S., 2006. Langmuir 22, 10152–10156.
Wang, J.L., Munir, A., Li, Z.H., Zhou, H.S., 2009. Biosens. Bioelectron. 25, 124–129.
Wang, Q., Yang, X.H., Wang, K.M., 2007. Sens. Actuators B Chem. 123, 227–232.
Wink, T., van Zuilen, S.J., Bult, A., van Bennekom, W.P., 1998. Anal. Chem. 70, 827–832.
Yang, X.H., Wang, Q., Wang, K.M., Tan, W.H., Li, H.M., 2007. Biosens. Bioelectron. 22, 1106–1110.
Yao, X., Li, X., Toledo, F., Zurita-Lopez, C., Gutova, M., Momand, J., Zhou, F.M., 2006. Anal. Biochem. 354, 220–228.
Yao, X., Wang, J.X., Zhou, F.M., Wang, J., Tao, N.J., 2004. J. Phys. Chem. B 108, 7206–7212.
Yao, X., Yang, M.L., Wang, Y.F., Hu, Z.B., 2007. Sens. Actuators B Chem. 122, 351–356.
Zauner, G., Wang, Y.T., Lavesa-Curto, M., MacDonald, A., Mayes, A.G., Bowater, R.P., Butt, J.N., 2005. Analyst 130, 345–349.